Momentum distribution function of the electron gas at metallic densities

Yasutami Takada
Institute for Solid State Physics, University of Tokyo, 7-22-1 Roppongi, Minato-ku, Tokyo 106, Japan

H. Yasuhara
College of General Education, Tohoku University, Sendai 980, Japan
(Received 11 April 1990; revised manuscript received 15 October 1990)

The momentum distribution function $n(k)$ of the electron gas is calculated in the effective-potential-expansion method at metallic densities. The recently established self-consistency relation between $n(k)$ and the correlation energy [Y. Takada and T. Kita, J. Phys. Soc. Jpn. **60**, 25 (1991)] is employed to check the accuracy of our results. This check shows that the effective-potential-expansion method provides probably the exact and at least more accurate results of $n(k)$ than all the other methods that have given $n(k)$ thus far.

I. INTRODUCTION

The electron gas has attracted attention for more than half a century partly because it provides an excellent testing ground for almost all many-body techniques and partly because the knowledge of its correlation energy per electron, ε_c, is essential for the local-density approximation[1] (LDA) on which many recent energy-band calculations are based. Although ε_c is now known accurately by the Green's-function Monte Carlo (GFMC) method,[2,3] we need as accurate information about the quasiparticle properties of the electron gas as we have about ε_c in order to construct an improved energy-band calculational scheme over the LDA. For the purpose of obtaining the quasiparticle properties, the GFMC method is not so useful because it produces large statistical errors particularly for quantities near the Fermi surface.

In this paper, we focus on the momentum distribution function $n(k)$ of the electron gas. $n(k)$ has been calculated by Daniel and Vosko[4] in the random-phase approximation (RPA). Later some of the exchange terms were included by Lam.[5] At about the same time, Overhauser[6] calculated $n(k)$ in his plasmon-pole approximation in which the exchange and the correlation effects were considered in terms of the so-called local-field correction in the definition of the static dielectric function. Lantto[7] made a Fermi hypernetted-chain (FHNC) calculation in which the short-range correlation is thought to be treated quite accurately. In a recent paper,[8] one of the present authors developed an improved version of the effective-potential expansion (EPX) method with which we can obtain new data on $n(k)$.

The results of $n(k)$ in these calculations do not agree. Thus we need some guiding principle based on which we can determine the superiority of one calculation to others. Recently a very useful self-consistency relation is established between $n(k)$ and ε_c.[9] Since we know the exact ε_c of the electron gas, we can use the self-consistency relation as the guiding principle by checking how precisely the relation is satisfied in each approximation for $n(k)$. We show the results of this check in this paper, together with those of $n(k)$ in various methods.

In Sec. II we give a formulation for $n(k)$ in the EPX method with a critical review of the calculations in both the Green's function and the FHNC approaches. In Sec. III we first recapitulate the self-consistency relation between $n(k)$ and ε_c and then give $n(k)$ in various methods. The accuracy of each calculation is checked with the self-consistency relation. At the end of the section, we discuss the magnitude of the discontinuity of $n(k)$ at the Fermi surface which is equal to the quasiparticle renormalization factor z_F. In Sec. IV we summarize our results. We discuss an appropriate formula for z_F in the RPA in an appendix. In this paper, we employ units in which $\hbar=1$.

II. FORMULATION

A. Hamiltonian

The homogeneous electron gas is a system consisting of N electrons embedded in a uniform positive-charge background. The electrons interact with one another through the Coulomb interaction. Thus the Hamiltonian is written in second quantization as

$$H=H_0+V\ , \tag{2.1}$$

where

$$H_0=\sum_{\mathbf{k}\sigma}\varepsilon_{\mathbf{k}}C^{\dagger}_{\mathbf{k}\sigma}C_{\mathbf{k}\sigma}\ , \tag{2.2}$$

and

$$V=\tfrac{1}{2}\sum_{\mathbf{q}\neq 0}\sum_{\mathbf{k}\sigma}\sum_{\mathbf{k}'\sigma'}V(q)C^{\dagger}_{\mathbf{k}+\mathbf{q}\sigma}C^{\dagger}_{\mathbf{k}'-\mathbf{q}\sigma'}C_{\mathbf{k}'\sigma'}C_{\mathbf{k}\sigma}\ , \tag{2.3}$$

with $\varepsilon_{\mathbf{k}}=\mathbf{k}^2/2m$ and $V(q)=4\pi e^2/q^2$. The volume of the system is taken to be unity. We specify an electron by momentum $\mathbf{k}$ and spin σ and represent its annihilation operator by $C_{\mathbf{k}\sigma}$. This system is described by a single parameter r_s, defined by $r_s\equiv me^2/\alpha k_F$ with α

$=(4/9\pi)^{1/3}=0.521$ and the Fermi momentum $k_F\equiv(3\pi^2N)^{1/3}$. In this paper, we consider r_s in the range 1–6.

B. Review of previous calculations

Daniel and Vosko[4] calculated $n(k)$ by evaluating the terms shown diagrammatically in Fig. 1. Those terms are expressed as

$$n(k)=\int_{-\infty}^{\infty}\frac{d\omega}{2\pi i}[G^{(0)}_{\mathbf{k}\sigma}(\omega)+G^{(0)}_{\mathbf{k}\sigma}(\omega)\Sigma^{(1)}_{\mathbf{k}\sigma}(\omega)G^{(0)}_{\mathbf{k}\sigma}(\omega)]\ , \tag{2.4}$$

where $G^{(0)}_{\mathbf{k}\sigma}(\omega)$ is the one-particle Green's function in the noninteracting system and $\Sigma^{(1)}_{\mathbf{k}\sigma}(\omega)$ is the first-order self-energy, given as

$$\Sigma^{(1)}_{\mathbf{k}\sigma}(\omega)=-\sum_{\mathbf{q}}\int_{-\infty}^{\infty}\frac{d\Omega}{2\pi i}G^{(0)}_{\mathbf{k}+\mathbf{q}\sigma}(\omega+\Omega)\frac{V(q)}{1+V(q)\Pi(q,\Omega)}\ . \tag{2.5}$$

Here $\Pi(q,\Omega)$ is the polarization function in the RPA. Transforming the Ω integral along the imaginary axis from the real axis,[10] we obtain

$$\begin{aligned}n(k)=n_{\mathbf{k}\sigma}-\sum_{\mathbf{q}}\int_0^{\infty}\frac{d\Omega}{\pi}&\frac{V(q)}{1+V(q)\Pi(q,i\Omega)}\\&\times\frac{\Omega^2-[\Delta(\mathbf{k};\mathbf{q})]^2}{\{\Omega^2+[\Delta(\mathbf{k};\mathbf{q})]^2\}^2}\\&\times[n_{\mathbf{k}\sigma}(1-n_{\mathbf{k}+\mathbf{q}\sigma})\\&\quad-n_{\mathbf{k}+\mathbf{q}\sigma}(1-n_{\mathbf{k}\sigma})]\ ,\end{aligned} \tag{2.6}$$

where $n_{\mathbf{k}\sigma}$ is equal to $\Theta(k_F-|\mathbf{k}|)$ with the Heaviside unit-step function $\Theta(x)$, $\Delta(\mathbf{k};\mathbf{q})$ is defined by

$$\Delta(\mathbf{k};\mathbf{q})\equiv|\varepsilon_{\mathbf{k}+\mathbf{q}}-\varepsilon_{\mathbf{k}}|\ , \tag{2.7}$$

and $\Pi(q,i\Omega)$ is calculated as

$$\Pi(q,i\Omega)=2\sum_{\mathbf{k}\sigma}\frac{n_{\mathbf{k}\sigma}(1-n_{\mathbf{k}+\mathbf{q}\sigma})\Delta(\mathbf{k};\mathbf{q})}{\Omega^2+[\Delta(\mathbf{k};\mathbf{q})]^2}\ . \tag{2.8}$$

Lam[5] included some of the exchange terms in addition to the terms in (2.6). In those calculations, however, the ladder diagrams which control the short-range correlation[11] are not considered. Thus we cannot expect reliable values for $n(k)$ at k much different from k_F where the short-range correlation involving large energy excitations plays a primary role in the determination of $n(k)$.

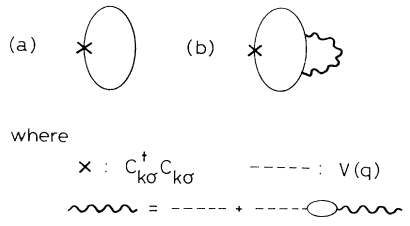

FIG. 1. Feynman diagrams for the calculation of $n(k)$ in the RPA of Daniel and Vosko (Ref. 4).

The short-range correlation is treated quite well in the variational theories based on the Jastrow wave function,[12] given by

$$|\Phi_0\rangle=\prod_{i<j}f(r_{ij})|0\rangle\ , \tag{2.9}$$

where $|0\rangle$ is a state described by the plane-wave Slater determinant and $f(r)$ is a two-particle correlation function. A scheme to evaluate the energy expectation value with respect to the trial function (2.9) is called the Fermi hypernetted-chain (FHNC) method[13] in which the variational parameter $f(r)$ is determined by the solution of the Euler-Lagrange-type equation. Lantto[7] made such a calculation and calculated $n(k)$ through

$$n(k)\equiv\langle\Phi_0|C^{\dagger}_{\mathbf{k}\sigma}C_{\mathbf{k}\sigma}|\Phi_0\rangle/\langle\Phi_0|\Phi_0\rangle\ . \tag{2.10}$$

The main problem in the choice of (2.9) is that the energy denominators like $\Delta(\mathbf{k};\mathbf{q})$ are not included. Basically, the energy denominators are very important in the evaluation of the correlation effect, or the deformation effect of the many-body wave function, in a system in which the Fermi level is located in the continuum of energy eigenvalues. Without the energy denominators, all the electrons are treated in the same way, irrespective of their location in the Fermi sphere. Although it may be permissible for the quantities like ε_c in which summations over all the electrons are done and also for $n(k)$ at k much different from k_F where the energies involved in the virtual transitions are large, the absence of the energy denominators may give a fatal error in $n(k)$ near $k=k_F$. We are afraid that near the Fermi surface the FHNC approach gives a smaller deviation of $n(k)$ from $n_{\mathbf{k}\sigma}$ than the exact value. This will result in a too large discontinuity of $n(k)$ at $k=k_F$ in this method.[9]

This absence of the energy denominators also causes a problem when the FHNC method is applied to the calculation of the quasiparticle properties in the system with the interaction having q^{-2} singularity. A physically correct screening behavior near $q=0$ can be obtained only when all the ring diagrams in the sense of the usual Green's-function method are summed as in (2.5). But the absence of the energy denominators makes the meaning of the ring diagrams defined in the FHNC theories a different one and thus the sum of those ring diagrams does not lead to a complete screening at $q=0$. The problem of the incomplete screening becomes serious for the quantities near the Fermi surface. In fact, Lantto[7] pointed out that his result of $n(k)$ had a logarithmically divergent derivative at the Fermi surface, though the result of $n(k)$ in (2.6) does not have such a behavior.

C. The EPX method

As we have discussed above, the Green's-function and the FHNC approaches are complementary to each other. The former has a favorable feature for the calculation of $n(k)$ near the Fermi surface, while the latter provides an

appropriate method for $n(k)$ at k much different from k_F. The EPX method is a combination of those perturbation-theoretic and variational theories. Thus it is expected to give $n(k)$ which is accurate enough in the whole region of k.

A trial function for the ground state in the EPX method is given with a correlation operator $U(0,-\infty)$ as[8]

$$|\Phi_0\rangle = U(0,-\infty)|0\rangle \equiv \sum_{n=0}^{\infty} \frac{1}{n!}\left[\sum_{m=1}^{\infty} U_m(0,-\infty)\right]^n |0\rangle , \tag{2.11}$$

where $U_m(0,-\infty)$ is defined as

$$U_m(0,-\infty) = \frac{(-i)^m}{m!}\int_{-\infty}^{0} e^{0^+t_1}dt_1 \ldots \int_{-\infty}^{0} e^{0^+t_m}dt_m\, T[\tilde{V}_l(t_1)\ldots\tilde{V}_l(t_m)]_L + \frac{(-i)^m}{(m-1)!}\int_{-\infty}^{0} e^{0^+t_1}dt_1 \ldots \int_{-\infty}^{0} e^{0^+t_m}dt_m\, T[\tilde{V}_s(t_1)\tilde{V}_l(t_2)\ldots\tilde{V}_l(t_m)]_L , \tag{2.12}$$

with the long- and the short-range parts of the effective potential $\tilde{V}_l$ and $\tilde{V}_s$. We do not explain either the meanings of the symbols in (2.12) or the physical considerations to reach this form here. Both of them were given in detail in Ref. 8.

We can write the energy expectation value E_0 with respect to $|\Phi_0\rangle$ as a power series in $\tilde{V}_s$ as

$$E_0 \equiv \langle\Phi_0|H|\Phi_0\rangle / \langle\Phi_0|\Phi_0\rangle = \sum_{n=0}^{\infty} E^{(n)} . \tag{2.13}$$

The nth-order term in (2.13) is given by the sum of the terms each of which is represented as a multidimensional integral of momentum variables for the integrand composed of n $\bar{V}_s(q)$'s and numbers of $\tilde{V}_l(q)$'s up to infinite order. Here $\bar{V}_s(q)$ is given by

$$\bar{V}_s(q) \equiv \frac{\tilde{V}_s(q)}{[\epsilon(q,0)]^2} , \tag{2.14}$$

with the dielectric function $\epsilon(q,\Omega)$, defined as

$$\epsilon(q,\Omega) = 1 + \Pi(q,\Omega)\tilde{V}_l(q) . \tag{2.15}$$

All the important terms in E_0 up to eighth order were given explicitly in Ref. 8. The optimum $\tilde{V}_l(q)$ and $\bar{V}_s(q)$ to give the minimum E_0 were determined in Ref. 8 and the results were shown in Fig. 5 of that paper. We note that $\tilde{V}_l(q)$ is optimized within a functional form, given by

$$\tilde{V}_l(q) = V(q)/[\tfrac{1}{2} + \tfrac{1}{2}\exp(q^2/q_c^2)] , \tag{2.16}$$

where the optimized cutoff momentum q_c was found to be less than $0.16k_F$ for r_s in the metallic densities. Thus $\tilde{V}_l(q)$ is not zero only for q less than about $0.2k_F$. On the other hand, $\bar{V}_s(q)$ is very small in that region.

We can use (2.10) for $n(k)$ with the trial function in (2.11). As in (2.13), $n(k)$ is expanded in powers of $\bar{V}_s(q)$ as

$$n(k) = \sum_{n=0}^{\infty} n^{(n)}(k) . \tag{2.17}$$

The terms in $n^{(0)}(k)$ are represented by the Feynman diagrams with the symbol $\times$ in Fig. 1 in Ref. 8. The Hartree term is given by $n_{\mathbf{k}\sigma}$ and the ring contribution $n_r^{(0)}(k)$ is expressed by the second term in (2.4) with $V(q)$ replaced by $\tilde{V}_l$. The exchange term is given by

$$n_{\rm ex}^{(0)}(k) = \sum_{\mathbf{q}\mathbf{q}'} \int_{-\infty}^{\infty}\frac{d\Omega}{2\pi i}\int_{-\infty}^{\infty}\frac{d\Omega'}{2\pi i}\int_{-\infty}^{\infty}\frac{d\omega}{2\pi i}\frac{\tilde{V}_l(q)}{\epsilon(q,\Omega)}\frac{\tilde{V}_l(q')}{\epsilon(q',\Omega')} \times G_{\mathbf{k}\sigma}^{(0)}(\omega)^2 G_{\mathbf{k}+\mathbf{q}'\sigma}^{(0)}(\omega+\Omega')G_{\mathbf{k}+\mathbf{q}\sigma}^{(0)}(\omega+\Omega)G_{\mathbf{k}+\mathbf{q}+\mathbf{q}'\sigma}^{(0)}(\omega+\Omega+\Omega') . \tag{2.18}$$

This contribution is very small. Namely, its absolute value is always less than one-hundredth of that of $n_r^{(0)}(k)$. The same is true for the contribution from the two other diagrams having two screened interactions $\tilde{V}_l/\epsilon$. The terms with more than two screened interactions have much less contribution. Thus $n^{(0)}(k)$ is given by (2.6) with $V(q)$ replaced by $\tilde{V}_l$.

The first-order ring contribution $n_r^{(1)}(k)$ is shown diagrammatically in Fig. 3(a_2) in Ref. 8. It can be expressed as the second term in (2.4) with $V(q)/[1+V(q)\Pi(q,\Omega)]$ replaced by $\tilde{V}_s/[\epsilon(q,\Omega)]^2$. We can employ the static approximation as explained in Ref. 8 for the calculation of $n_r^{(1)}(k)$. As a result, it is written as

$$n_r^{(1)}(k) = -2\sum_{\mathbf{q}}\sum_{\mathbf{k}'\sigma'}\frac{\tilde{V}_l(q)}{\epsilon(q,0)}\bar{V}_s(q)\frac{n_{\mathbf{k}'\sigma'}(1-n_{\mathbf{k}'-\mathbf{q}\sigma'})}{[\Delta(\mathbf{k};\mathbf{q})+\Delta(\mathbf{k}';-\mathbf{q})]^2}[n_{\mathbf{k}\sigma}(1-n_{\mathbf{k}+\mathbf{q}\sigma})-n_{\mathbf{k}+\mathbf{q}\sigma}(1-n_{\mathbf{k}\sigma})] . \tag{2.19}$$

The product of $\bar{V}_s(q)$ with $\bar{V}_l(q)/\epsilon(q,0)$ is small in the entire region of q. Thus the contribution of $n_r^{(1)}(k)$ is not large,

i.e., about one-tenth of that of $n_r^{(0)}(k)$. Further, there is a strong cancellation of this term with the exchange term shown in Fig. 3(b_2) in Ref. 8. Therefore, $n^{(1)}(k)$ contributes very little to $n(k)$.

The important contribution to $n^{(2)}(k)$ comes only from the two diagrams in Fig. 4(a) in Ref. 8. The static approximation can be used to evaluate those terms. Then the combination of them gives $n^{(2)}(k)$ as

$$n^{(2)}(k)=-\sum_{\mathbf{q}}\sum_{\mathbf{k}'\sigma'}\bar{V}_s(q)[\bar{V}_s(q)\epsilon(q,0)-\delta_{\sigma\sigma'}\bar{V}_s(|\mathbf{k}'-\mathbf{k}-\mathbf{q}|)] \times\frac{n_{\mathbf{k}'\sigma'}(1-n_{\mathbf{k}'-\mathbf{q}\sigma'})[n_{\mathbf{k}\sigma}(1-n_{\mathbf{k}+\mathbf{q}\sigma})-n_{\mathbf{k}+\mathbf{q}\sigma}(1-n_{\mathbf{k}\sigma})]}{[\Delta(\mathbf{k};\mathbf{q})+\Delta(\mathbf{k}';-\mathbf{q})]^2} . \tag{2.20}$$

The overall behavior of $n(k)$ is almost determined by the sum of (2.20) and the Hartree term $n_{\mathbf{k}\sigma}$. In particular, only (2.20) determines the deviation of $n(k)$ from $n_{\mathbf{k}\sigma}$ at k much different from k_F.

Among the higher-order terms, odd-power contributions can be neglected for the same reason as explained for the first-order term. However, we have to include even-power contributions, especially those from the fourth- and the sixth-order ring families. We can employ the same approximation for the calculation of those terms in $n^{(2n)}(k)$ as that for $E_r^{(2n)}(H_0)$ given in Ref. 8. The result is given by

$$\begin{aligned}n^{(2n)}(k)=-\sum_{\mathbf{q}}\sum_{\mathbf{k}_2\sigma_2}\cdots\sum_{\mathbf{k}_{2n}\sigma_{2n}}&[\bar{V}_s(q)]^{2n-2}[\epsilon(q,0)]^{2n-4}\\ &\times\{[\bar{V}_s(q))]^2[\epsilon(q,0)]^3-[(2n-2)\delta_{\sigma_2\sigma_3}\bar{V}_s(|\mathbf{k}_2-\mathbf{k}_3-\mathbf{q}|)\\ &\qquad+2\epsilon(q,0)\delta_{\sigma\sigma_2}\bar{V}_s(|\mathbf{k}-\mathbf{k}_2+\mathbf{q}|)]\epsilon(q,0)\bar{V}_s(q)\\ &+\delta_{\sigma\sigma_2}\delta_{\sigma\sigma_{2n}}[2n-3+2\epsilon(q,0)]\bar{V}_s(|\mathbf{k}-\mathbf{k}_{2n}+\mathbf{q}|)\bar{V}_s(|\mathbf{k}-\mathbf{k}_2+\mathbf{q}|)\}\\ &\times\frac{n_{\mathbf{k}_2\sigma_2}(1-n_{\mathbf{k}_2-\mathbf{q}\sigma_2})\ldots n_{\mathbf{k}_{2n}\sigma_{2n}}(1-n_{\mathbf{k}_{2n}-\mathbf{q}\sigma_{2n}})}{[\Delta(\mathbf{k};\mathbf{q})+\Delta(\mathbf{k}_2;-\mathbf{q})][\Delta(\mathbf{k}_2;-\mathbf{q})+\Delta(\mathbf{k}_3,\mathbf{q})]\ldots[\Delta(\mathbf{k}_{2n};-\mathbf{q})+\Delta(\mathbf{k};\mathbf{q})]}\\ &\times[n_{\mathbf{k}\sigma}(1-n_{\mathbf{k}+\mathbf{q}\sigma})-n_{\mathbf{k}+\mathbf{q}\sigma}(1-n_{\mathbf{k}\sigma})] ,\end{aligned} \tag{2.21}$$

for $n=2,3,\ldots$.

III. CALCULATED RESULTS

A. Self-consistency relation

Based on the Pauli-Feynman theorem,[14] we can derive an exact relation between $n(k)$ and $E_0(\lambda)$ which is the ground-state energy of the system described by the Hamiltonian $H(\lambda)\equiv H_0+\lambda V$ with a scaling parameter λ. According to Ref. 9, the relation is given by

$$\sum_{\mathbf{k}\sigma}\varepsilon_{\mathbf{k}}n(k)=E_0(1)-\left.\frac{\partial E_0(\lambda)}{\partial\lambda}\right|_{\lambda=1} . \tag{3.1}$$

In the electron gas, $E_0(\lambda)$ is usually expressed as

$$E_0(\lambda)=\frac{me^4}{2}\lambda^2 N\left[\frac{2.21}{\lambda^2 r_s^2}-\frac{0.916}{\lambda r_s}+\varepsilon_c(\lambda r_s)\right] , \tag{3.2}$$

where $\varepsilon_c(\lambda r_s)$ is the correlation energy per electron as a function of the scaled r_s parameter λr_s. In terms of the difference between $n(k)$ and $n_{\mathbf{k}\sigma}$, (3.1) is rewritten as

$$\frac{me^4}{2}N\Delta\varepsilon_t(r_s)\equiv\sum_{\mathbf{k}\sigma}\varepsilon_{\mathbf{k}}[n(k)-n_{\mathbf{k}\sigma}] =\frac{me^4}{2}N\left[-\varepsilon_c-r_s\frac{d\varepsilon_c}{dr_s}\right] . \tag{3.3}$$

Here $\Delta\varepsilon_t(r_s)$ may be regarded as the kinetic-energy shift per electron in units of Rydberg (Ry) $me^4/2$. It is positive definite by its definition. Since ε_c and its derivative with respect to r_s are known very accurately,[2,3] we can give the accurate value of $\Delta\varepsilon_t(r_s)$ for each value of r_s from the right-hand side of (3.3). In Table I, we give those values of $\Delta\varepsilon_t(r_s)$ for a very wide range of r_s.

Equation (3.3) is very useful for the check of accuracy of $n(k)$: If we obtain $n(k)$ in some approximate calculation, we can evaluate its accuracy by comparing between the accurate value of $\Delta\varepsilon_t(r_s)$ and that from the left-hand side of (3.3). The conservation of the total number of electrons leads to another relation for $n(k)$ as

$$\sum_{\mathbf{k}\sigma}[n(k)-n_{\mathbf{k}\sigma}]=0 . \tag{3.4}$$

However, this is not so useful, because almost all the approximate calculations for $n(k)$ satisfy (3.4) automatically. Thus (3.4) can be used only for the check of the numerical calculation rather than the validity of the approximation.

B. Momentum distribution function

In Fig. 2 we show the calculated results of $n(k)$ in various methods at $r_s=4$. The solid, the dashed, the dotted, and the dashed-dotted curves represent, respectively, the results in the EPX method, the FHNC of Lantto,[7] the

TABLE I. Kinetic-energy shift per electron $\Delta\varepsilon_t$ for various values of r_s in units of Ry.

	r_s							
	1	2	3	4	5	6	10	20
$\Delta\varepsilon_t$	0.0733	0.0486	0.0368	0.0296	0.0248	0.0212	0.0132	0.006 40

RPA of Daniel and Vosko,[4] and a correction to the RPA with some of the exchange terms given by Lam.[5] The result obtained by Overhauser[6] is very close to that of Lam at this value of r_s. (This is an accidental coincidence. For other values of r_s, they are not the same. The result of Overhauser seems to be much better than that of Lam as we will see later.) Since the correlation effect is overestimated in the calculation of Daniel and Vosko, its result of $n(k)$ gives a too large deviation from the noninteracting value $n_{k\sigma}$ in the whole region of k. A considerable improvement seems to be made by Lam. In particular, the Lam result happens to be very close to that in the EPX method near the Fermi surface at this value of r_s. At k much different from k_F, however, the Lam result is not good at all. For those values of k, the FHNC method gives essentially the same result as that in the EPX method. In fact, these two are different only in the very vicinity of the Fermi surface.

In order to find the best $n(k)$ among those results, we have calculated $\Delta\varepsilon_t(r_s)$ through the left-hand side of (3.3). The values for $\Delta\varepsilon_t(4)$ are, respectively, obtained as 0.0549, 0.0432, 0.0271, and 0.0292 Ry per electron for $n(k)$ in the RPA, the Lam theory, the FHNC approach, and the EPX method. On the other hand, the exact value for $\Delta\varepsilon_t(4)$ is given as 0.0296 Ry per electron as shown in Table I. Thus the EPX method gives the best value and is very close to the exact result. Note that if we calculate $n(k)$ up to second order in (2.17), we obtain 0.0273 Ry for $\Delta\varepsilon_t(4)$. If we consider the situation from the side of the FHNC method, we can conclude that the overall behavior of $n(k)$ is quite good due to a correct treatment of the short-range correlation. To get a better agreement with the correct value of $\Delta\varepsilon_t(4)$, i.e., to have a larger kinetic-energy shift by about 9%, $n(k)$ near the Fermi surface should be a little more deviated from $n_{k\sigma}$ as we have obtained in the EPX method.

We have also calculated $\Delta\varepsilon_t$ at other values of r_s. In Fig. 3, the results of $\Delta\varepsilon_t$ with $n(k)$ in the EPX method

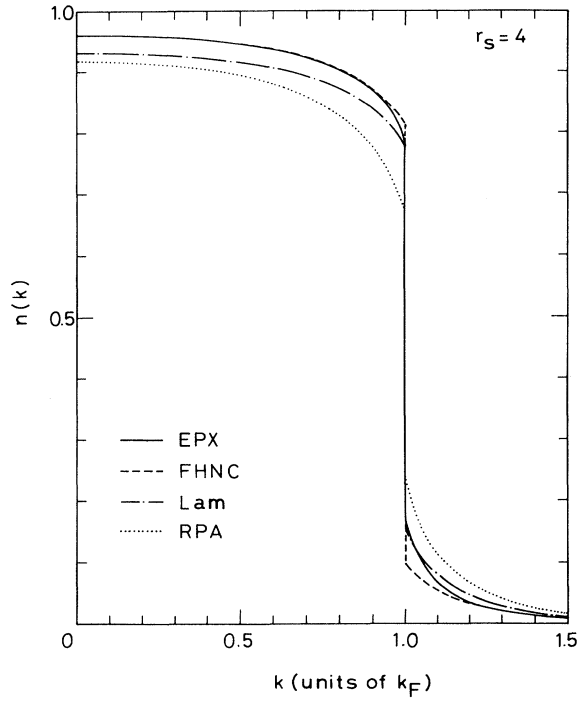

FIG. 2. Calculated results of $n(k)$ of the electron gas in various methods at $r_s=4$. The solid, the dashed, the dotted, and the dashed-dotted curves represent, respectively, the results in the EPX, the FHNC (Ref. 7), the RPA (Ref. 4), and a correction to the RPA with some of the exchange terms (Ref. 5).

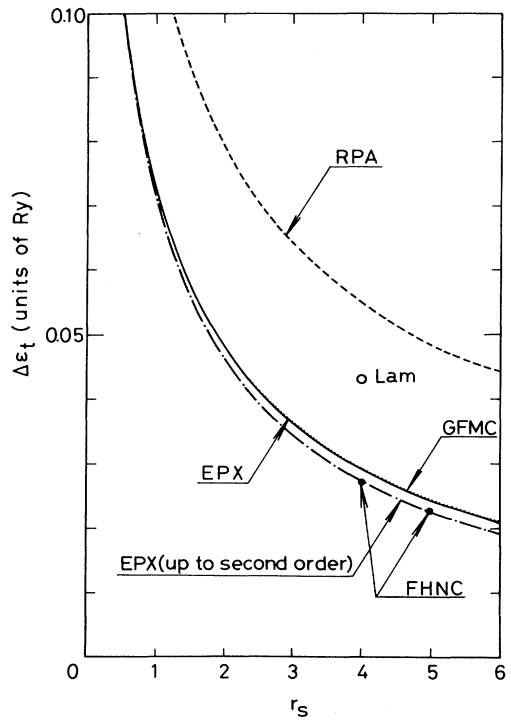

FIG. 3. Kinetic-energy shift per electron in Ry units as a function of r_s. The results of $\Delta\varepsilon_t$ with $n(k)$ in the EPX method are given by the solid curve. The results with $n(k)$ up to second order in (2.17) are shown by the dotted-dashed curve. The dotted and the dashed curves represent, respectively, the exact values in Table I determined with the use of the GFMC method (Refs. 2 and 3) and those with $n(k)$ in the RPA (Ref. 4). The results in the FHNC method (Ref. 7) and the Lam theory (Ref. 5) are shown by the solid and the open circles, respectively.

are given by the solid curve. Since the results are very close to the exact ones in Table I plotted by the dotted curve, it is difficult to distinguish the two curves on the scale of this figure. For comparison, the results with $n(k)$ up to second order in (2.17) are shown by the dotted-dashed curve, while those with $n(k)$ in the RPA are given by the dashed curve. The results in the FHNC method and the Lam theory are shown by the solid and the open circles, respectively. The FHNC results happen to be on the dotted-dashed curve.

Since the EPX method seems to give the values of $n(k)$ very close to the exact ones, it may be useful to show the results of $n(k)$ for other values of r_s. In Fig. 4, we plot $n(k)$ for $r_s=1$, 3, and 5. When k becomes very large compared to k_F, $n(k)$ behaves as[15]

$$n(k)=0.0122r_s^2 g_{\uparrow\downarrow}(0)\left[\frac{k_F}{k}\right]^8 , \tag{3.5}$$

where $g_{\uparrow\downarrow}(0)$ is the spin-antiparallel pair distribution function at zero separation. We find that $n(k)$ in the EPX method shows this asymptotic behavior for k larger than about $4k_F$. The values for $g_{\uparrow\downarrow}(0)$ obtained from (3.5) are, respectively, 0.54, 0.17, and 0.055 for $r_s=1$, 3, and 5. Of course, these values agree with those given by the solid curve in Fig. 9 of Ref. 16.

The fractional number of electrons excited above the Fermi surface by the correlation effect $\Delta N/N$, is defined by

$$\Delta N/N \equiv \int_0^{k_F} dk \frac{[1-n(k)]3k^2}{k_F^3} . \tag{3.6}$$

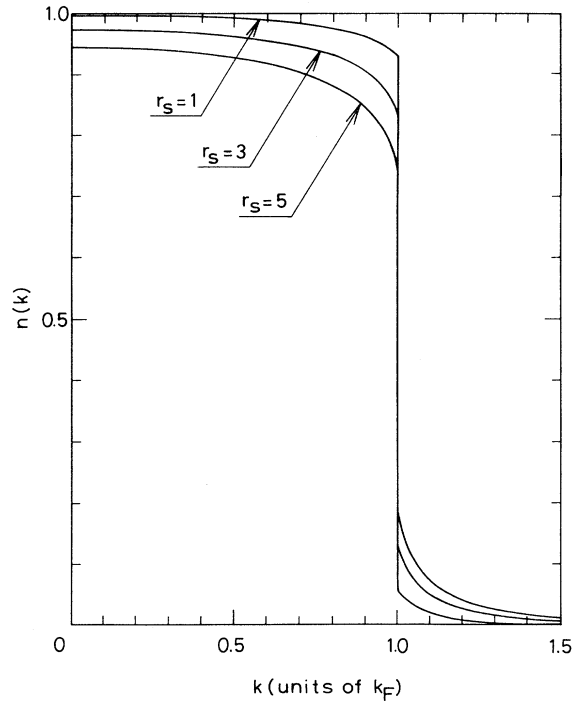

FIG. 4. Results of $n(k)$ in the EPX method for $r_s=1$, 3, and 5.

The calculated results of $\Delta N/N$ in the EPX method, the RPA, and the Overhauser theory are, respectively, plotted as a function of r_s in Fig. 5 by the solid, the dashed, and the dotted curves. The two solid circles represent the results in the FHNC method.

C. Quasiparticle renormalization factor at the Fermi surface

As shown in Figs. 2 and 4, $n(k)$ has a discontinuity at $k=k_F$. Its magnitude is related to the renormalization factor at the Fermi surface z_F.[17] In Fig. 6 we show the r_s dependence of z_F obtained from various calculations of $n(k)$. The solid, the dashed, the dotted, the dashed-dotted, and the dashed–double dotted curves correspond, respectively, to the results in the EPX method, the FHNC approach, the RPA of Daniel and Vosko, the Lam theory, and the Overhauser plasmon-pole approximation. Although it provides quite good results for the quantities like $\Delta N/N$ in which all the electrons are involved, the FHNC method gives a rather poor result for z_F in which only the electrons near the Fermi surface play a primary role. Thus it seems certain that for the quantities like z_F the inclusion of the energy denominators in the trial function is quite important. On the other hand, the Overhauser result is very close to that of the EPX method in the whole region of r_s, though the values for $\Delta N/N$ are quite different between the two. This indicates that even if $n(k)$ in the entire region of k is not always correct we can obtain a correct $n(k)$ near the Fermi surface as long as the screening behavior is treated correctly combined with proper sum rules.

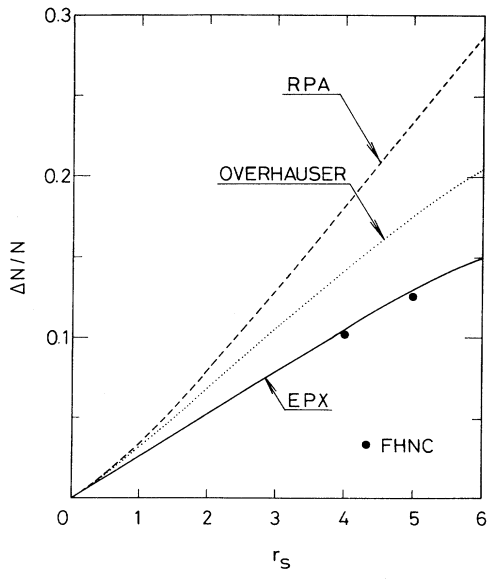

FIG. 5. Fractional number of electrons excited above the Fermi surface. The results in the EPX method, the RPA (Ref. 4), and the Overhauser plasmon-pole approximation (Ref. 6) are, respectively, plotted as a function of r_s by the solid, the dashed, and the dotted curves. The two solid circles represent the results in the FHNC method.

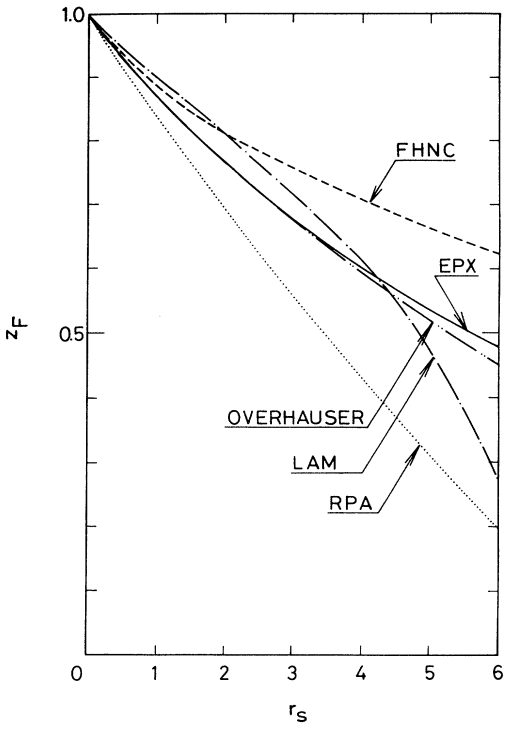

FIG. 6. Renormalization factor at the Fermi surface as a function of r_s obtained from the magnitude of the discontinuity of $n(k)$ at $k=k_F$. The solid, the dashed, the dotted, the dashed-dotted, and the dashed–double dotted curves correspond, respectively, to the results in the EPX method, the FHNC theory (Ref. 7), the RPA (Ref. 4), the Lam theory (Ref. 5), and the Overhauser plasmon-pole approximation (Ref. 6).

In the Green's-function method,[10,18] we can go beyond the calculation in (2.4), if we confine ourselves to the properties near the Fermi surface. For the calculation of z_F, for example, we can sum infinite number of terms shown in Fig. 7 instead of two in Fig. 1. The result for z_F obtained from such a calculation is

$$z_F=\left[1-\frac{\partial\Sigma^{(1)}_{\mathbf{k}\sigma}(\varepsilon_{\mathbf{k}})}{\partial\varepsilon_{\mathbf{k}}}\bigg|_{|\mathbf{k}|=k_F}\right]^{-1}, \tag{3.7}$$

while the result indicated by the RPA in Fig. 6 is

$$z_F=1+\frac{\partial\Sigma^{(1)}_{\mathbf{k}\sigma}(\varepsilon_{\mathbf{k}})}{\partial\varepsilon_{\mathbf{k}}}\bigg|_{|\mathbf{k}|=k_F}. \tag{3.8}$$

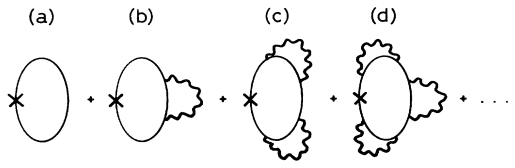

FIG. 7. Feynman diagrams for the calculation of $n(k)$ obtained by the infinite sum of the RPA terms in Fig. 1.

In Fig. 8 we compare the results of z_F in (3.7) with those in (3.8) as a function of r_s, together with those in the EPX method shown in Fig. 6. As can be seen, (3.7) and (3.8) give very different z_F.

In the literature,[10,18] formula (3.7) is usually employed for the calculation of z_F. However, it is physically quite puzzling that (3.7) in the RPA gives a larger value than (the probably correct) z_F in the EPX method for $r_s>2$, because the important corrections to the RPA are considered to make z_F larger. Therefore we have reconsidered the applicability of (3.7). The details of the discussion are given in the Appendix, but our conclusion is that the correct value of z_F in the RPA is given by (3.8) (the dotted curve in Fig. 8) rather than (3.7). Formula (3.7) includes some effects of the exchange and the ladder diagrams implicitly and this is the reason why (3.7) gives a value of z_F much closer to that in the EPX method than (3.8).

IV. SUMMARY

Based on the self-consistency relation between the momentum distribution function $n(k)$ and the correlation energy, we have verified that the EPX method gives quite accurate results for $n(k)$ of the electron gas at metallic densities. We have also argued that both the short-

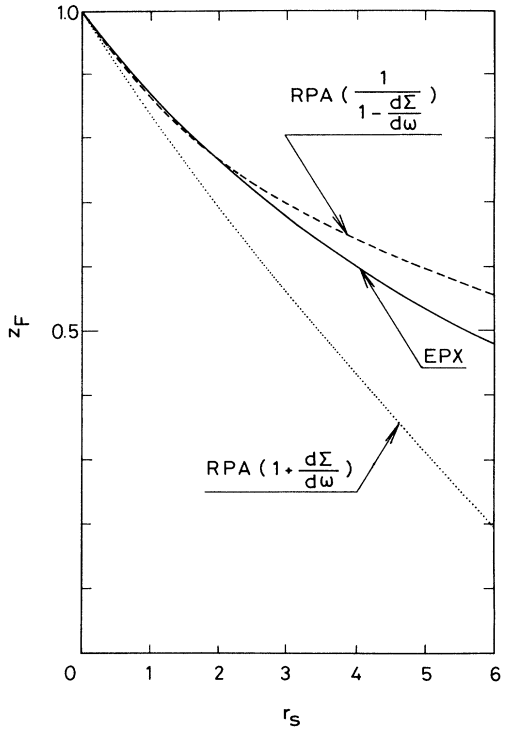

FIG. 8. Renormalization factor z_F as a function of r_s calculated in the RPA in two different formulas. The dotted and dashed curves give, respectively, the results of the formulas to first order (3.8) and to infinite order (3.7). The results in the EPX method are plotted by the solid curve and are the same as in Fig. 6.

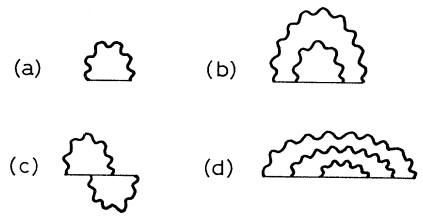

FIG. 9. Feynman diagrams for $\Sigma^{(1)}_{k\sigma}(\omega)$, $\Sigma^{(2s)}_{k\sigma}(\omega)$, $\Sigma^{(2ex)}_{k\sigma}(\omega)$, and $\Sigma^{(3s)}_{k\sigma}(\omega)$. They are given in (a), (b), (c), and (d), respectively.

and the long-range correlation should be treated accurately in order to obtain the correct behavior of $n(k)$ in the whole region of k. The former plays a primary role in the region of k much different from k_F, while the latter plays a role in that of k near the Fermi surface. Among the calculations of $n(k)$ reported thus far, only the EPX method includes both of these effects correctly. As a by-product of this study, we have reconsidered the conventional formula (3.7) for z_F and clarified the implication of the formula.

APPENDIX: RENORMALIZATION FACTOR IN THE RPA

Basically, $n(k)$ can be calculated by the ω integral of the full Green's function $G_{k\sigma}(\omega)$ as

$$n(k)=\int_{-\infty}^{\infty}\frac{d\omega}{2\pi i}G_{k\sigma}(\omega)$$
$$=\int_{-\infty}^{\infty}\frac{d\omega}{2\pi i}\left[G^{(0)}_{k\sigma}(\omega)^{-1}-\Sigma_{k\sigma}(\omega)\right]^{-1}, \quad \text{(A1)}$$

where $\Sigma_{k\sigma}(\omega)$ is the full self-energy. The true energy dispersion ω_k is determined by

$$\omega_k=\varepsilon_k+\Sigma_{k\sigma}(\omega_k)\ , \quad \text{(A2)}$$

and z_F is given by

$$z_F=\left[1-\frac{\partial\Sigma_{k\sigma}(\omega_k)}{\partial\omega_k}\bigg|_{|k|=k_F}\right]^{-1}. \quad \text{(A3)}$$

Now we expand $\Sigma_{k\sigma}(\omega)$ as

$$\Sigma_{k\sigma}(\omega)=\Sigma^{(1)}_{k\sigma}(\omega)+\Sigma^{(2s)}_{k\sigma}(\omega)+\Sigma^{(2ex)}_{k\sigma}(\omega)+\cdots\ , \quad \text{(A4)}$$

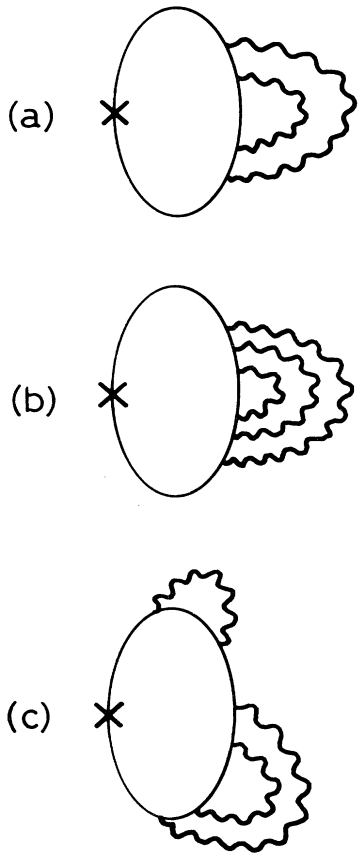

FIG. 10. Examples of the Feynman diagrams for the self-energy corrections to $n(k)$.

where $\Sigma^{(1)}_{k\sigma}(\omega)$, $\Sigma^{(2s)}_{k\sigma}(\omega)$, and $\Sigma^{(2ex)}_{k\sigma}(\omega)$ are given diagrammatically in Figs. 9(a), 9(b), and 9(c). [The expression for $\Sigma^{(1)}_{k\sigma}(\omega)$ is given in (2.5).] Up to second order of this expansion, (A2) is solved as

$$\omega_k=\varepsilon_k+\Sigma^{(1)}_{k\sigma}(\varepsilon_k)+\frac{\partial\Sigma^{(1)}_{k\sigma}(\varepsilon_k)}{\partial\varepsilon_k}\Sigma^{(1)}_{k\sigma}(\varepsilon_k)$$
$$+\Sigma^{(2s)}_{k\sigma}(\varepsilon_k)+\Sigma^{(2ex)}_{k\sigma}(\varepsilon_k)\ . \quad \text{(A5)}$$

As noted by DuBois,[19] there is a strong cancellation between the third and the fourth terms in (A5). In fact, the sum is given by

$$\frac{\partial\Sigma^{(1)}_{k\sigma}(\varepsilon_k)}{\partial\varepsilon_k}\Sigma^{(1)}_{k\sigma}(\varepsilon_k)+\Sigma^{(2s)}_{k\sigma}(\varepsilon_k)=\sum_{qq'}\int_{-\infty}^{\infty}\frac{d\Omega}{2\pi i}\int_{-\infty}^{\infty}\frac{d\Omega'}{2\pi i}G^{(0)}_{k+q\sigma}(\varepsilon_k+\Omega)^2G^{(0)}_{k+q'\sigma}(\varepsilon_k+\Omega')\frac{V(q)}{1+V(q)\Pi(q,\Omega)}$$
$$\times\left[\frac{V(|q'-q|)}{1+V(|q'-q|)\Pi(|q'-q|,\Omega'-\Omega)}-\frac{V(q')}{1+V(q')\Pi(q',\Omega')}\right], \quad \text{(A6)}$$

and it becomes very small. Similar cancellations also occur in higher-order terms as well. Thus as far as we calculate the self-energy in terms of the bare Green's function as in (2.5), it is sensible to calculate ω_k by

$$\omega_k=\varepsilon_k+\Sigma_{k\sigma}(\varepsilon_k)\ . \quad \text{(A7)}$$

In particular, if we neglect all the exchange diagrams such as $\Sigma_{\mathbf{k}\sigma}^{(2\mathrm{ex})}(\varepsilon_{\mathbf{k}})$ we can replace the self-energy by $\Sigma_{\mathbf{k}\sigma}^{(1)}(\varepsilon_{\mathbf{k}})$ in (A7).

In the same spirit, we can rewrite (A3) up to second order as

$$z_F^{-1}=1-\frac{\partial\Sigma_{\mathbf{k}\sigma}^{(1)}(\varepsilon_{\mathbf{k}})}{\partial\varepsilon_{\mathbf{k}}}-\frac{\partial^2\Sigma_{\mathbf{k}\sigma}^{(1)}(\varepsilon_{\mathbf{k}})}{\partial\varepsilon_{\mathbf{k}}^2}\Sigma_{\mathbf{k}\sigma}^{(1)}(\varepsilon_{\mathbf{k}})-\frac{\partial\Sigma_{\mathbf{k}\sigma}^{(2s)}(\varepsilon_{\mathbf{k}})}{\partial\varepsilon_{\mathbf{k}}}-\frac{\partial\Sigma_{\mathbf{k}\sigma}^{(2\mathrm{ex})}(\varepsilon_{\mathbf{k}})}{\partial\varepsilon_{\mathbf{k}}}$$
$$=1-\frac{\partial\Sigma_{\mathbf{k}\sigma}^{(1)}(\varepsilon_{\mathbf{k}})}{\partial\varepsilon_{\mathbf{k}}}+\left[\frac{\partial\Sigma_{\mathbf{k}\sigma}^{(1)}(\varepsilon_{\mathbf{k}})}{\partial\varepsilon_{\mathbf{k}}}\right]^2-\frac{\partial\Sigma_{\mathbf{k}\sigma}^{(2\mathrm{ex})}(\varepsilon_{\mathbf{k}})}{\partial\varepsilon_{\mathbf{k}}}-\partial\left[\frac{\partial\Sigma_{\mathbf{k}\sigma}^{(1)}(\varepsilon_{\mathbf{k}})}{\partial\varepsilon_{\mathbf{k}}}\Sigma_{\mathbf{k}\sigma}^{(1)}(\varepsilon_{\mathbf{k}})+\Sigma_{\mathbf{k}\sigma}^{(2s)}(\varepsilon_{\mathbf{k}})\right]\Big/\partial\varepsilon_{\mathbf{k}}\ , \tag{A8}$$

with $|\mathbf{k}|$ evaluated at k_F. As before, we can neglect the last term in (A8). Then we obtain (3.8) instead of (3.7) for z_F up to second order, if we do not include the exchange diagrams. Similar cancellations work in higher-order terms. For example, when we include the third-order term $\Sigma_{\mathbf{k}\sigma}^{(3s)}(\omega)$ as shown in Fig. 9(d), we obtain up to third order as

$$z_F^{-1}=1-\frac{\partial\Sigma_{\mathbf{k}\sigma}^{(1)}(\varepsilon_{\mathbf{k}})}{\partial\varepsilon_{\mathbf{k}}}+\left[\frac{\partial\Sigma_{\mathbf{k}\sigma}^{(1)}(\varepsilon_{\mathbf{k}})}{\partial\varepsilon_{\mathbf{k}}}\right]^2-\left[\frac{\partial\Sigma_{\mathbf{k}\sigma}^{(1)}(\varepsilon_{\mathbf{k}})}{\partial\varepsilon_{\mathbf{k}}}\right]^3\ , \tag{A9}$$

where we have considered the cancellation between $\Sigma_{\mathbf{k}\sigma}^{(2s)}(\omega)\partial\Sigma_{\mathbf{k}\sigma}^{(1)}(\omega)/\partial\omega$ and $\Sigma_{\mathbf{k}\sigma}^{(3s)}(\omega)$. In a diagrammatic language, we can say that the self-energy corrections to $n(k)$ in Fig. 10 cancel the contribution of higher-order ring terms for $n(k)$ in Fig. 7. For example, the term in Fig. 7(c) is cancelled by the one in Fig. 10(a). Therefore we find that (3.8) gives the result for z_F in the RPA with all the terms in Figs. 1, 7, and 10 and thus it is superior to (3.7). Note that this is consistent with the conventional procedure[10] to calculate the effective mass m^* by the derivative of $\omega_{\mathbf{k}}$ in (A7) with respect to k. Note also that if the exchange term $\Sigma_{\mathbf{k}\sigma}^{(2\mathrm{ex})}$ is included and its derivative happens to cancel the third term in the last line of (A8), we obtain (3.7) for z_F. This indicates that the formula (3.7) includes implicitly some effect of the terms which are not included in the RPA.

[1]For reviews, see, for example, W. Kohn and P. Vashishta, in *Theory of the Inhomogeneous Electron Gas,* edited by S. Lundqvist and N. H. March (Plenum, New York, 1983), p. 79 and *Many-Body Phenomena at Surfaces,* edited by D. Langreth and H. Suhl (Academic, Orlando, 1984), Chap. 1.

[2]D. M. Ceperley and B. J. Alder, Phys. Rev. Lett. **45**, 566 (1980).

[3]S. H. Vosko, L. Wilk, and M. Nusair, Can. J. Phys. **58**, 1200 (1980).

[4]E. Daniel and S. H. Vosko, Phys. Rev. **120**, 2041 (1960).

[5]J. Lam, Phys. Rev. B **3**, 3243 (1971).

[6]A. W. Overhauser, Phys. Rev. B **3**, 1888 (1971).

[7]L. J. Lantto, Phys. Rev. B **22**, 1380 (1980).

[8]Y. Takada, Phys. Rev. B **43**, 5962 (1991).

[9]Y. Takada and T. Kita, J. Phys. Soc. Jpn. **60**, 25 (1991).

[10]T. M. Rice, Ann. Phys. (N.Y.) **31**, 100 (1965).

[11]K. S. Singwi, M. P. Tosi, R. H. Land, and A. Sjölander, Phys. Rev. **176**, 589 (1968); H. Yasuhara, Solid State Commun. **11**, 1481 (1972).

[12]R. Jastrow, Phys. Rev. **98**, 1479 (1955).

[13]For a review in relation to the electron gas, see E. Krotscheck, Ann. Phys. (N.Y.) **155**, 1 (1984).

[14]R. P. Feynman, Phys. Rev. **56**, 340 (1939).

[15]J. C. Kimball, J. Phys. A **8**, 1513 (1975); H. Yasuhara and Y. Kawazoe, Physica **85A**, 416 (1976).

[16]Y. Takada, Phys. Rev. B **35**, 6923 (1987).

[17]A. B. Migdal, Zh. Exp. Teor. Fiz. **32**, 399 (1957) [Sov. Phys. JETP **5**, 333 (1957)].

[18]L. Hedin. Phys. Rev. **139**, A796 (1965); L. Hedin and S. Lundqvist, in *Solid State Physics,* edited by F. Seitz, D. Turnbull, and H. Ehrenreich (Academic, New York, 1969), Vol. 23, p. 1.

[19]D. F. DuBois, Ann. Phys. (N.Y.) **7**, 174 (1959); **8**, 24 (1959).